

Technical Notes

TECHNICAL NOTES are short manuscripts describing new developments or important results of a preliminary nature. These Notes cannot exceed 6 manuscript pages and 3 figures; a page of text may be substituted for a figure and vice versa. After informal review by the editors, they may be published within a few months of the date of receipt. Style requirements are the same as for regular contributions (see inside back cover).

Two-Stream Mixing: A Variational Solution

R. D. Small*

*Technion-Israel Institute of Technology,
Haifa, Israel*

Nomenclature

- $a(x)$ = velocity profile shift
 E^* = local potential
 n = exponent
 L = length
 u, v = velocity components in x and y directions, respectively
 U = average initial velocity $(U_1 + U_2)/2$
 U_1 = velocity at $y = +\infty$
 U_2 = velocity at $y = -\infty$
 x, y = Cartesian coordinates
 δ = variational operator
 ϵ, ϵ_0 = eddy viscosity
 η = similarity coordinate ($\eta = 1/2 y \sqrt{U/\nu x}$)
 $\tilde{\eta}$ = similarity coordinate ($\tilde{\eta} = 1/2 [y + a(x)] \sqrt{U/\nu x}$)
 λ = relative velocity parameter [$\lambda = (U_1 - U_2)/(U_1 + U_2)$]
 ν = viscosity
 ρ = density
 Φ = error function
 ψ = stream function

I. Introduction

THE mixing of two initially semi-infinite uniform streams (cf. Fig. 1) of different velocities is the simplest representation of the general problem of viscous mixing. To first order, the boundary-layer equations adequately describe the physical mixing process, since viscosity predominates in a region of small thickness as compared to the length of the mixing process, and, likewise, the normal velocity v is small as compared to the velocity in the flow direction u .

Solutions¹⁻⁴ of the boundary-layer equations for the mixing of two initially uniform streams have been obtained for a variety of physical cases including laminar and turbulent mixing of incompressible and compressible flows, and mixing of two streams of different composition. In general, solution procedures for laminar and turbulent flows are similar if an eddy viscosity $\epsilon = \epsilon_0 (x/L)^n$ is used.

Analytic solutions thus far obtained are inaccurate or nonunique⁵ as the boundary-layer equations reduce to a third-order equation, whereas the physical problem allows definition of only two boundary conditions, i.e., $u \rightarrow U_1$ as $y \rightarrow +\infty$ and $u \rightarrow U_2$ as $y \rightarrow -\infty$. A third boundary condition necessary to specify completely the problem must be assumed and usually is taken to be $\psi = 0$ or $u = (U_1 + U_2)/2$ on $y = 0$. Obviously neither of these assumptions is strictly correct. As a

result, the calculated profiles, while correct functionally, are not located properly in the flowfield.

In the following analysis, the concept of the local potential or generalized entropy production as developed by Glansdorff and Prigogine⁶ is used to provide a third condition and an analytic solution is obtained for the incompressible laminar mixing of two initially uniform streams of different velocities. The solution obtained shows excellent agreement with the numerical results of Lock.³

II. Analysis

The equation for the local potential or generalized entropy production can be written as⁷

$$E^* = \int_0^L \int_{-\infty}^{\infty} \left[u \left(\frac{\partial u^0}{\partial x} \right)^2 - u^0 v^0 \frac{\partial u}{\partial y} + \nu \frac{\partial u^0}{\partial y} \frac{\partial u}{\partial y} - \frac{1}{2} (u^2 + v^2) \left(\frac{\partial u^0}{\partial x} + \frac{\partial v^0}{\partial y} \right) + \frac{u}{\rho} \frac{\partial p}{\partial x} \right] dy dx + \oint \left(u^0 v^0 u - \nu u \frac{\partial u^0}{\partial y} \right) dx \quad (1)$$

The superscripted values represent properties of the stationary state, and the region of integration is defined by the control volume shown in Fig. 1. The problem is to find the extremum of E^* such that it is minimum. For the case of constant pressure mixing and since the shear stress vanishes at $y = \pm \infty$, Eq. (1) reduces to

$$E^* = \int_0^L \int_{-\infty}^{\infty} \left[u \left(\frac{\partial u^0}{\partial x} \right)^2 - u^0 v^0 \frac{\partial u}{\partial y} + \nu \frac{\partial u^0}{\partial y} \frac{\partial u}{\partial y} \right] dy dx + \oint u^0 v^0 u dx \quad (2)$$

The procedure at this point is to select a trial function for $u(x, y)$, take the variation of E^* , and then use the auxiliary conditions $u = u^0$ and $v = v^0$.

Görtler¹ and Pai⁸ have shown, and it is generally recognized, that the profile after mixing can, to first order, be represented by an error function, i.e.,

$$u = U(1 + \lambda \text{erf} \eta) \quad (3)$$

where $U = (U_1 + U_2)/2$, $\lambda = (U_1 - U_2)/(U_1 + U_2)$, and $\eta = y/2 \sqrt{U/\nu x}$. The third boundary condition used in

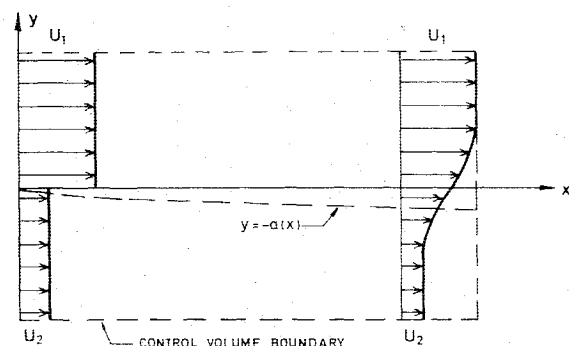


Fig. 1 Two-stream mixing.

Received March 18, 1977. Copyright © American Institute of Aeronautics and Astronautics, Inc., 1977. All rights reserved.

Index categories: Jets, Wakes, and Viscid-Inviscid Flow Interactions; Boundary Layers and Convective Heat Transfer—Laminar.

*Senior Lecturer, Department of Aeronautical Engineering, Member AIAA.

deriving this profile is that $u=U$ on $y=0$. In general, $u=U$ will occur at a location other than $y=0$, e.g., $y=-a(x)$, where $a(0)=0$, and $a(x)$ should depend parametrically on U_1 and U_2 or λ . $a(x)$ represents a shift in the location of the error function profile.

Accordingly, the following form of u is assumed:

$$u = U(1 + \lambda \operatorname{erf} \bar{\eta}) \quad (4)$$

where

$$\bar{\eta} = \frac{1}{2}[y + a(x)]\sqrt{U/\nu x} \quad (5)$$

The boundary conditions $u \rightarrow U_1$, $y \rightarrow \infty$; $u \rightarrow U_2$, $y \rightarrow -\infty$ are satisfied, and, on $y = -a(x)$, $u = U$. It can be shown (from continuity) that, with the preceding form of u , then

$$v = -U\lambda[a'(x)\operatorname{erf} \bar{\eta} - \frac{1}{2}\sqrt{U/\nu x} (e^{-\bar{\eta}^2} - 1)/\sqrt{\pi}] \quad (6)$$

It remains to find the best functional form (via minimization of E^*) of $a(x)$ subject to $a(0)=0$.

Substitution of Eq. (4) into Eq. (2) and taking the variation of E^* with respect to $a(x)$, holding all superscript quantities constant during variation, yields

$$\delta E^* = \frac{U\lambda}{\sqrt{\pi}} \int_0^L \sqrt{\frac{U}{\nu x}} \int_{-\infty}^{\infty} \left\{ \frac{\partial}{\partial x} (u^{u^2}) + \left(\frac{U}{\nu x} \right) \frac{y+a(x)}{2} \left[u^u v^v - \nu \frac{\partial u^u}{\partial y} \right] \right\} e^{-\bar{\eta}^2} \delta a dy dx \quad (7)$$

Using the auxiliary conditions $u = u^u$, $v = v^v$ and substituting Eqs. (4) and (6) into Eq. (7), yields

$$\delta E^* = \frac{\lambda^2 U^3}{\sqrt{\pi}} \int_0^L \frac{U}{\nu x} \int_{-\infty}^{\infty} \left[a' \Phi' - \frac{7}{8} \frac{y+a}{x} \Phi' + \lambda a' \Phi' \Phi - \frac{5}{8} \frac{y+a}{x} \lambda \Phi' \Phi + \frac{1}{\sqrt{\pi}} \frac{y+a}{4x} (1 + \lambda \Phi) - a' \sqrt{\frac{U}{\nu x}} \left(\frac{y+a}{2} \Phi + \lambda \frac{y+a}{2} \Phi^2 \right) \right] e^{-\bar{\eta}^2} \delta a dy dx \quad (8)$$

where $\Phi(\bar{\eta}) = \operatorname{erf} \bar{\eta}$, $\Phi' = \partial \Phi / \partial \bar{\eta}$, and $a' = (\partial / \partial x) a(x)$. Integration over y and setting δE^* to zero in order to find the extremum results in

$$0 = \int_0^L \frac{1}{x} \left\{ a'(x) \sqrt{2} \sqrt{\frac{Ux}{\nu}} + \frac{\lambda}{2\sqrt{\pi}} \left(\sqrt{2} - \frac{5}{\sqrt{3}} \right) \right\} dx \quad (9)$$

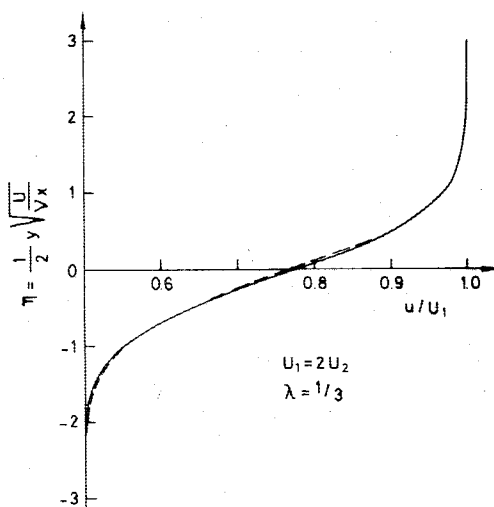


Fig. 2 Shear layer velocity profile: solid curve, Eq. (13); dashed curve, numerical solution.³

Table 1 Profile location

U_2/U_1	λ	$y\sqrt{U_1/\nu x}$	$(u/U_1)_{y=0}$	$(u/U_1)_{y=0}(\text{Ref. 1})$
0.66667	0.2000	-0.12871	0.84436	0.83333
0.50000	0.33333	-0.22611	0.77753	0.75000
0.33333	0.50000	-0.35974	0.72148	0.66666
0.25000	0.60000	-0.44585	0.69879	0.62500
0.20000	0.66666	-0.50560	0.68725	0.60000
0.14286	0.75000	-0.58285	0.67612	0.57143
0.11111	0.8000	-0.63053	0.67111	0.55556
0.0	1.0	-0.83079	0.66107	0.50000

If δE^* is to be zero for arbitrary variations, then the integrand must vanish, and

$$a'(x) \sqrt{\frac{2Ux}{\nu}} + \frac{\lambda}{2\sqrt{\pi}} \left(\sqrt{2} - \frac{5}{\sqrt{3}} \right) = 0 \quad (10)$$

$a(x)$ is now determined via integration [using $a(0)=0$] to be

$$a(x) = \frac{5/\sqrt{6} - 1}{\sqrt{\pi}} \lambda \sqrt{\frac{\nu x}{U}} \quad (11)$$

and, accordingly,

$$\bar{\eta} = \frac{1}{2} \left(y + \frac{5/\sqrt{6} - 1}{\sqrt{\pi}} \lambda \sqrt{\frac{\nu x}{U}} \right) \sqrt{\frac{U}{\nu x}} \quad (12a)$$

$$\bar{\eta} = \eta + 0.29373\lambda \quad (12b)$$

The function $a(x)$ serves to locate properly the error function profile. It is proportional to \sqrt{x} and dependent on the initial relative velocity of the two streams. The velocity components can now be written as

$$u/U = 1 + \lambda \operatorname{erf}(\eta + 0.29373\lambda) \quad (13)$$

$$v/U = -(\lambda/2\sqrt{\pi}) \sqrt{\nu/Ux} [1.0412 \lambda \operatorname{erf}(\eta + 0.29373\lambda) + e^{-\bar{\eta}^2} - 1] \quad (14)$$

III. Results

The velocity profile as calculated from Eq. (13) is shown in Fig. 2 for the case of $U_2/U_1 = 1/2$, $\lambda = 1/3$. The present results show excellent agreement with the numerical solution of Lock.³ Values of the shift of the profile $y = -a(x)$, i.e., the values of y for which the boundary condition $u = U$ is valid, are listed in Table 1, as is u/U_1 on $y=0$. For comparison, values of u/U_1 as obtained from Görtler's¹ solution are listed in the last column.

It should be expected that the results for $\lambda \rightarrow 1$ are somewhat less exact, as the convergence of Görtler's series is better for $\lambda < 1$. However, it has been found both analytically and experimentally⁹ that the error function well describes the shear layer velocity profile. The choice of the error function is not necessary, and for the region $\lambda \sim 1$ a polynomial approximation or series of exponential functions can also be used.

IV. Concluding Remarks

A variational analysis has been used to find a solution for the mixing of two initially uniform streams of different velocities. The concept of the local potential was used to provide an additional condition, so that an analytic solution could be obtained. A number of boundary-layer-type problems have been solved^{10,12} using variational methods, and additional problems in which an approximate analytical solution is desired also can be solved using this method.

References

- ¹Görtler, H., Berechnung von Aufgaben der Freien Turbulenz auf Grund eines neuen Näherungsansatzes," *Zeitschrift für angewandte Mathematik und Mechanik*, Vol. 22, Oct. 1942, pp. 244-254.
- ²Pai, S. I., "Two-Dimensional Jet Mixing of a Compressible Fluid," *Journal of the Aeronautical Sciences*, Vol. 16, Aug. 1949, pp. 463-469.
- ³Lock, R. C., "The Velocity Distribution in the Laminar Boundary Layer Between Parallel Streams," *Quarterly Journal of Mechanics and Applied Mathematics*, Vol. IV, Pt. 1, 1951, pp. 42-63.
- ⁴Crane, L. J., "The Laminar and Turbulent Mixing of Jets of Compressible Fluid, Part II: The Mixing of Two Semi-Infinite Streams," *Journal of Fluid Mechanics*, Vol. 3, 1957, pp. 81-92.
- ⁵Ting, L., "On the Mixing of Parallel Streams," *Journal of Mathematics and Physics*, Vol. 38, 1959, pp. 153-165.
- ⁶Glansdorff, P. and Prigogine, I., "On a General Evolution Criterion in Macroscopic Physics," *Physica*, Vol. 30, 1964, pp. 351-374.
- ⁷Weih, D. and Gal-Or, B., "General Variational Analysis of Hydrodynamic, Thermal and Diffusional Boundary Layers," *International Journal of Engineering Science*, Vol. 8, 1970, pp. 231-249.
- ⁸Pai, S. I., "The Jet Mixing Region of an Incompressible Fluid," *Viscous Flow Theory*, Van Nostrand, New York, 1956, pp. 189-191.
- ⁹Korst, H. H., Page, R. H., and Childs, M. E., "Compressible Two-Dimensional Jet Mixing at Constant Pressure," Univ. of Illinois, ME-TN 392-1, 1954.
- ¹⁰Schechter, R. S., *The Variational Method in Engineering*, McGraw-Hill, New York, 1967, Chap. 5.
- ¹¹Doty, R. T. and Blick, E. F., "Local Potential Variational Method Applied to Hiemenz Flow," *AIAA Journal*, Vol. 11, June 1973, pp. 880-881.
- ¹²Weih, D., "On the Polynomial Approximation of Boundary-Layer Flow Profiles," *Applied Scientific Research*, Vol. 31, 1975, pp. 253-266.

Elliptical Water Jets

J. W. Hoyt*

U.S. Naval Academy, Annapolis, Md.

and

J. J. Taylor†

Naval Ocean Systems Center, San Diego, Calif.

Introduction

STUDIES of elliptical water jets have a very considerable history. In 1879 Lord Rayleigh¹ described tests on water jets discharging from elliptical orifices, and referred to earlier tests made "many years ago" by Bidone. Both Bidone and Rayleigh noticed the rather remarkable change with axial distance in the cross section of jets from elliptical orifices. If the major axis of the ellipse is, say, in the horizontal plane at the nozzle, in a short distance downstream the jet has changed so that its major axis is vertical.

This change in jet shape has been nicely sketched by Sir Geoffrey Taylor,² who also studied elliptic jets, and an adaptation of Taylor's sketch is given in Fig. 1. In the absence of surface tension, as in a gaseous jet, this is the final geometry of the jet, but, if surface tension is present, additional cycles are possible, the jet alternately switching major and minor axis cross sections.

Both Rayleigh and Taylor suggest that the change of shape of elliptic jets is due to the flow from the outer portions of the

ellipse (on the major axis) converging together in the manner of two circular jets impinging at a shallow angle; the resulting flatness at 90 deg to the ellipse major axis being due to the impingement. Indeed, Taylor² used an elliptical orifice flow to model the impinging circular-jet flow situation.

Applications of elliptic jets are not common, but they are occasionally found in heating and ventilating outlets and in ejectors. Nonaxisymmetric nozzles are sometimes employed in high-performance aircraft, because of the noise reduction aspects attributed to the "flat" sides of the jet (as discussed by Crighton³) or because of better geometrical adaptation to the complete aircraft design.⁴ Rectangular nozzles of the type occasionally installed in aircraft produce elliptical-shaped jets complete with 90-deg major axis shift. The present study was motivated by the desire to study elliptic jet flows as an interesting and little understood class of fluid phenomena, and by the hope that using high-speed photography, any changes

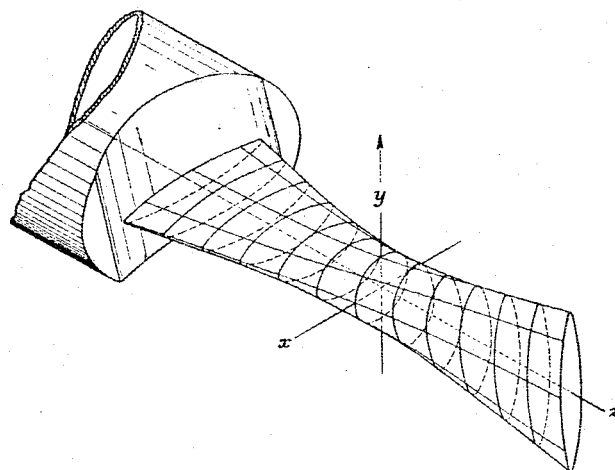
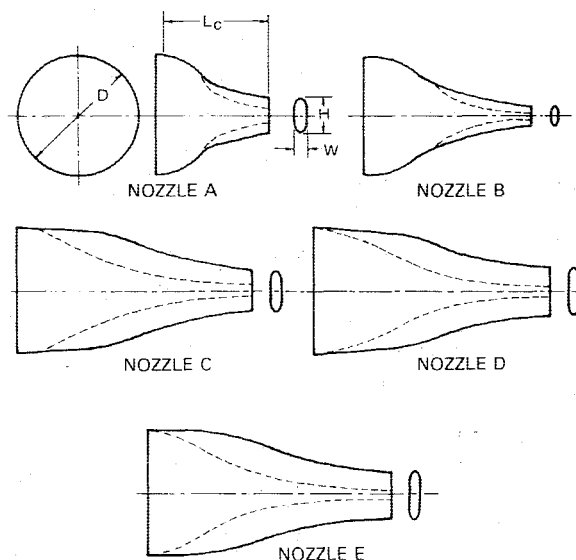


Fig. 1 Diagram of jet issuing from an elliptic orifice (after Taylor²).



NOZZLE DIMENSIONS, INCHES

NOZZLE	W	H	H/W	L _c	D	CONTRACTION RATIO
A	0.215	0.545	2.53	1.6	1.85	28.9
B	0.117	0.312	2.67	2.3	1.75	83.8
C	0.185	0.705	3.81	4.0	2.15	35.5
D	0.174	0.719	4.13	3.5	1.90	28.8
E	0.150	0.718	4.79	3.6	1.80	30.0

Fig. 2 Sketch of internal dimensions of nozzles used in the study (dashed lines show projections perpendicular to minor axis of ellipse).

Received June 6, 1977; revision received Sept. 27, 1977. Copyright © American Institute of Aeronautics and Astronautics, Inc., 1977. All rights reserved.

Index categories: Jets, Wakes, and Viscid-Inviscid Flow Interactions; Nozzle and Channel Flow.

*Professor, Naval Systems Engineering Dept.; presently at Naval Ocean Systems Center, San Diego.

†Consultant.